1

Physics Motivation

1.1 Why ^{3}He nuclei?

The ^{3}He nucleus is the subject of considerable current interest. It consists of two protons and a neutron. Being a three nucleon system makes it an ideal case for testing our understanding of the nuclear forces between nucleons, the structure of the nuclear ground state and the reaction mechanisms. It is complex enough to exhibit all important features that are present in the reactions with heavier nuclei. It allows us to study the effects such as Final State Interactions (FSI) and the Meson Exchange Currents (MEC). On the other hand it is small enough to be an exactly calculable nuclear system, where theoretical predictions of its nuclear structure can be compared with the experimental data to an increasingly accurate degree [1].

Consisting of three nucleons, ^{3}He is also an ideal candidate for studying three-nucleon forces (3NF). A need for inclusion of 3NF effects has been clearly demonstrated in calculations of ^{3}H and ^{3}He binding energies [2], where correct values are achieved only if 3NF is added. When using only nucleon-nucleon forces, binding energies of both nuclei are underestimated.

As an alternative to ^{3}He, ^{3}H nuclei could be considered for testing few-body theories. Since triton has exactly opposite structure then helium (^{3}He(ppn) $\rightarrow$ ^{3}H(nnp)), comparison of the two would give even further insight into the underlying theories. Unfortunately ^{3}H is radioactive, which prevents it from being explored in modern experiments, due to the safety concerns.

1.2 Structure of the ^{3}He nuclei

Theoretical calculations [3, 4] of the three-body bound state predict, that three components dominate the ^{3}He ground-state wave-function. See Fig. 1.1 and Table 1.1. The dominant component of the ^{3}He wave function is a spatially symmetric S state, in which the proton spins are in the spin-singlet state (anti-parallel) and the ^{3}He spin is predominantly carried by the neutron. This configuration accounts for $\approx$ 90 % of the spin-averaged wave function. The dominance of this state is supported by the fact, that the magnetic momentum of the ^{3}He is very close to the magnetic momentum of

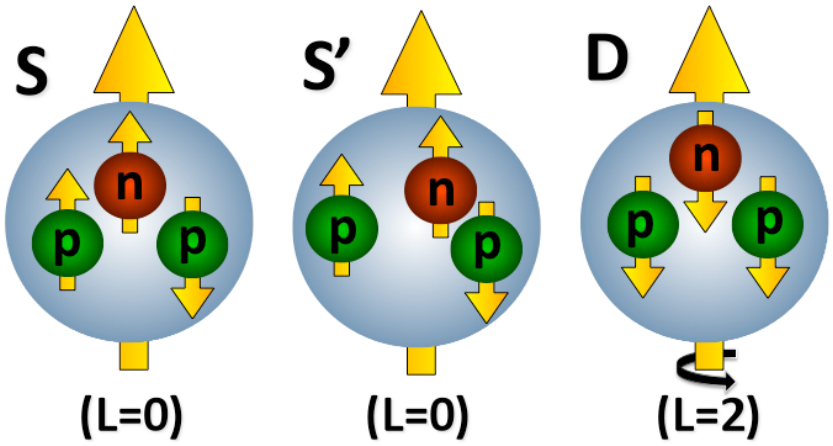

Figure 1.1 — Three dominant components (S, S′ and D) of the ^{3}He ground-state wave-function. Arrows show the spin orientations of the nucleons and nuclei, while L denotes the orbital angular momentum.

Table 1.1 — The partial wave channels of the three-nucleon (α, β, γ) wave function within the Derrick-Blatt scheme [3]. S and L are the spin and the angular momentum of ^{3}He. l_α is the relative orbital angular momentum of the pair ($\beta\gamma$), while L_α represents the orbital angular momentum of the ($\beta\gamma$) center of mass relative to α, with $\vec{L} = \vec{l}_\alpha + \vec{L}_\alpha$. P and K label the basis vectors $|PK\rangle$ of the irreducible representations of the permutation group S_3, which are considered for description of the three-nucleon spin states.

Channel number	L	S	l_α	L_α	P	K	Probability (%)	WF State
1	0	0.5	0	0	A	1	87.44	S
2	0	0.5	2	2	A	1	1.20	S
3	0	0.5	0	0	M	2	0.74	S′
4	0	0.5	1	1	M	1	0.74	S′
5	0	0.5	2	2	M	2	0.06	S′
6	1	0.5	1	1	M	1	0.01	P
7	1	0.5	2	2	A	1	0.01	P
8	1	0.5	2	2	M	2	0.01	P
9	1	1.5	1	1	M	1	0.01	P
10	1	1.5	2	2	M	2	0.01	P
11	2	1.5	0	2	M	2	1.08	D
12	2	1.5	1	1	M	1	2.63	D
13	2	1.5	1	3	M	1	1.05	D
14	2	1.5	2	0	M	2	3.06	D
15	2	1.5	2	2	M	2	0.18	D
16	2	1.5	3	1	M	1	0.37	D

the neutron [5]:

$$\frac{\mu_{^3\mathrm{He}}}{\mu_n} = \frac{-2.131}{-1.913} \approx 1$$

An additional $\approx 8\,\%$ of the spin-averaged wave-function can be attributed to the D state generated by the tensor component of the nucleon-nucleon force. In this case, the three nucleon spins are predominantly oriented opposite to the ^{3}He nuclear spin. The remaining $\approx 2\,\%$ originate from a mixed-symmetry configuration of the nucleons, the S′ state. It arises because of the differences between the isoscalar ($T = 0$) and isovector ($T = 1$) forces and hence reflects (spin-isospin)-space correlations [7]. The results of Faddeev calculations predict [2, 8], that the probability for S′ state depends on the binding energy of the nuclei and scales approximately as $P_{S'} \approx (E_{Binding}/\mathrm{MeV})^{-2.1}$. The S′ state does not exist for ^{2}H, whereas for ^{4}He and heavier nuclei it is expected to be strongly suppressed, with $P_{S'} < 0.1\,\%$. This makes ^{3}He and ^{3}H the only two nuclei, where S′ state can be observed. Estimated probabilities for finding nuclei in this state are $P_{^3He} = 1.24\,\%$ and $P_{^3H} = 1.05\,\%$. Hence, different probabilities for the S′ state in ^{3}He and ^{3}H explain the bulk of the difference between their charge radii ($r_{^3He} \approx 1.7$ fm, $r_{^3H} \approx 1.5$ fm) [9].

The contributions from other components of the ^{3}He ground-state wave-function (e.g. P-state) are estimated to be very small and can be neglected.

Understanding the role of the D and S′ states in ^{3}He is a very important aspect of the few-body theory. In particular, the observables that are sensitive to the S′ state constitute a stringent test of the quality of the theoretical calculations.

1.3 $^3\vec{\mathrm{He}}$ as an effective $\vec{n}$ target

A detailed knowledge of the ground-state spin structure of ^{3}He is very important also for extracting precise information on neutron structure. While the properties of the proton are nowadays well known and precisely measured, the structure of the neutron is not yet understood to a desirable accuracy. The most uncertain is the information about the neutron charge distribution. Fig. 1.2 shows the calculated values of the charge distributions for both proton and neutron [10]. The proton charge density is determined with an accuracy better than 8 %, while neutron charge density is known only with an accuracy of about 25 %. There is a continuous effort among the nuclear society to measure neutron property more precisely. However, the problem is, that direct measurements are not possible, because there is no neutron target. The structure of the neutron must therefore be determined indirectly. For that we use scattering experiments on the deuterium target, where we can assume that the neutron behaves almost as a free particle due to the small binding energy of the deuteron. As an effective polarized neutron target, a polarized ^{3}He can be used, by exploiting the fact, that the spin of the ^{3}He is essentially carried by the neutron.

1.3.1 Measurement of G_E^n form factor

The neutron charge distribution is determined through the measurement of the neutron electric form factor (G_E^n). Fig. 1.3 shows the majority of the available data for the G_E^n, obtained from the experiments using polarized deuterium ($^2\vec{\mathrm{H}}$) and polarized helium ($^3\vec{\mathrm{He}}$) targets. When utilizing polarized ^{3}He target, G_E^n is determined from the

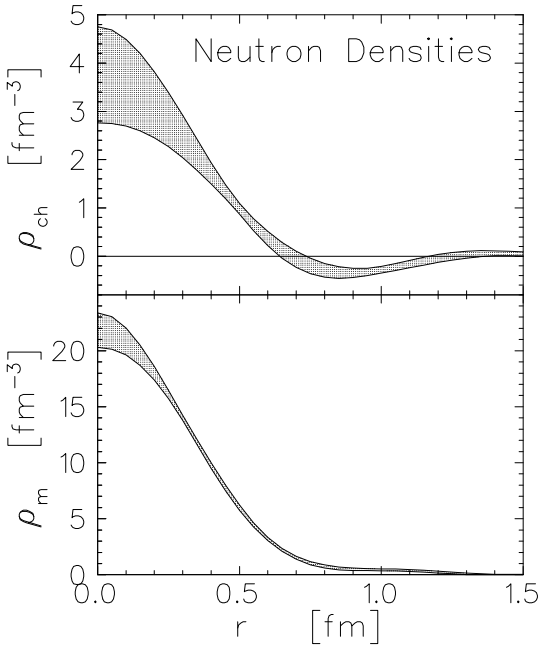

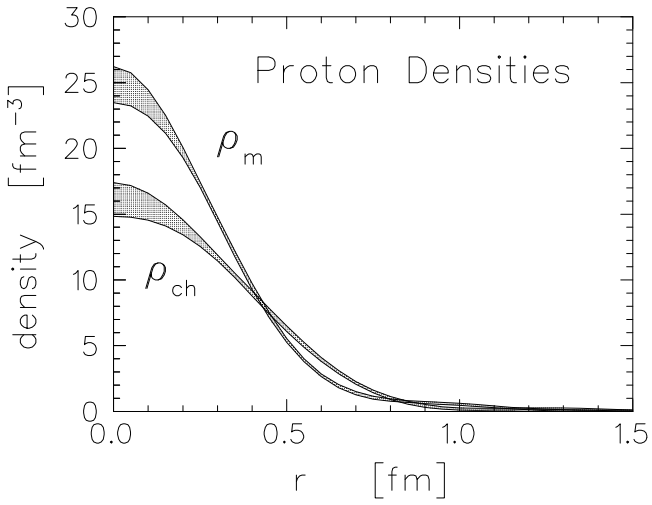

Figure 1.2 — Charge (ρ_{cm}) and magnetization (ρ_m) densities for the neutron (left) and proton (right) [10].

measurements of double polarized asymmetries in quasi-elastic processes $^3\vec{\mathrm{He}}\,(\vec{e}, e'n)$, $^3\vec{\mathrm{He}}\,(\vec{e}, e')$. To extract a precise information on the neutron electromagnetic form factors from these data, it is crucial to understand the ground-state spin structure of the ^{3}He nucleus in details. The importance of accurate theoretical description is illustrated in Fig. 1.3. The cyan arrow shows the size of a theoretical correction needed to properly interpret the Becker $^3\vec{\mathrm{He}}\,(\vec{e}, e'n)$ datum at $Q^2 = 0.35\,(\mathrm{GeV}/c)^2$ as effective neutron data [11]. This clearly shows, that a satisfactory description of the scattering process $^3\vec{\mathrm{He}}\,(\vec{e}, e'n)$ can no longer be provided by the plane-wave calculation, where ^{3}He is assumed to be only in a S-state and spin of the nuclei carried completely by the neutron. Instead, state-of-the-art Faddeev calculations are used, which consider full ^{3}He ground-state wave function, together with the reaction-mechanism effects such as final-state interactions (FSI) and meson-exchange currents (MEC). The differences between the plane-wave approximation and Faddeev calculations are significant, especially at low values of the Q^2, where the effects of the FSI for this process are most prominent. According to Fig. 1.3 the discrepancy exceeds the presently achievable experimental uncertainties by almost factor of three.

1.3.2 Measurement of G_M^n form factor

The ^{3}He target was extensively used also for determination of the magnetic form-factor of the neutron (G_M^n), which is intimately connected to the magnetization distribution inside the neutron (see Fig. 1.2). The G_M^n is extracted from the measurement of the double-polarization asymmetry $A_{T'}$ in the inclusive $^3\vec{\mathrm{He}}\,(\vec{e}, e')$ reaction. Fig. 1.4 shows results of such measurement performed at Jefferson Lab [12]. These experiments again relay on a fact, that in the ground state of ^{3}He, proton spins cancel each other out, and polarized ^{3}He behaves as an effective neutron target. However, the results show, that PWIA alone does not provide an adequate descriptions. Corrections for FSI and MEC have to be applied, which once more require a precise theoretical insight into the ^{3}He

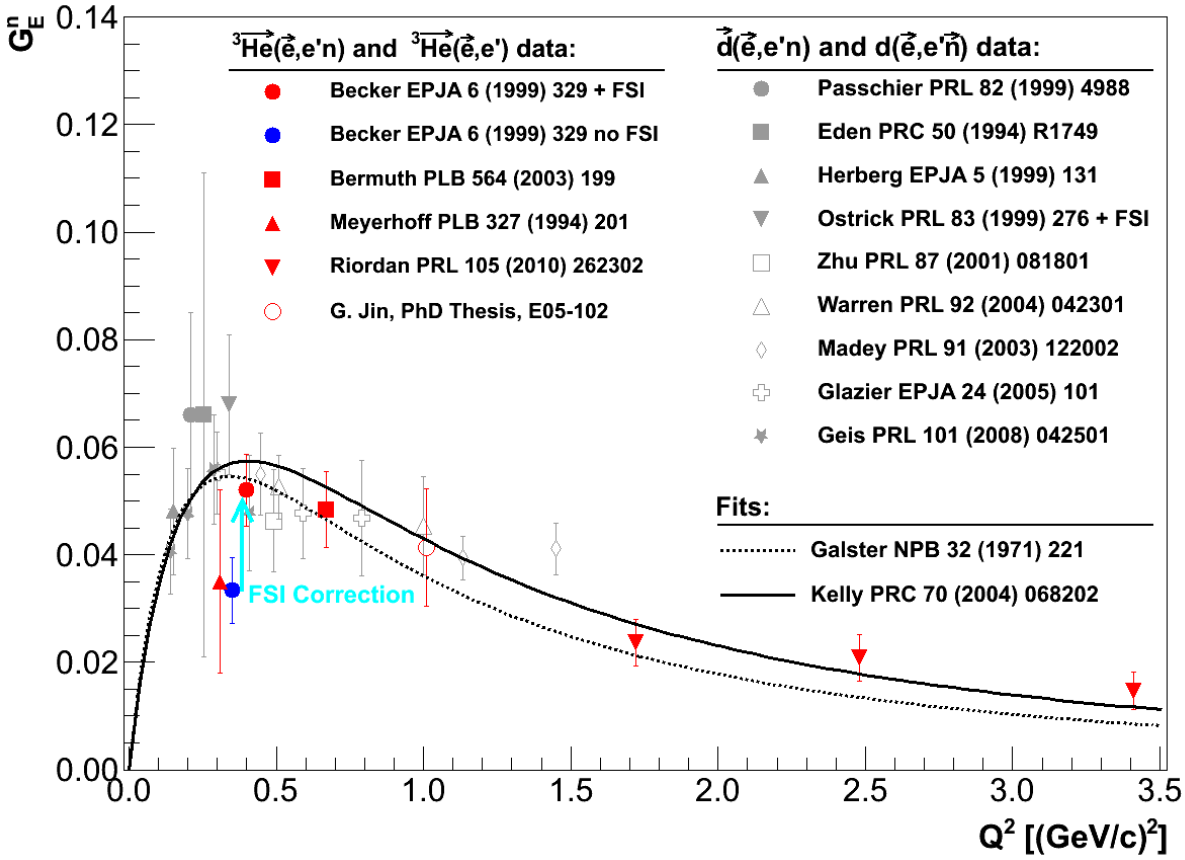

Figure 1.3 — Current status of extractions of G_E^n. Color points show results obtained from the cross-section asymmetries from polarized $^3\vec{He}$ target. The gray points are from the analysis of the cross-section asymmetries using a polarized $^2\vec{H}$ target. Full and dashed line represent the Kelly and Galster fit to G_E^n. Full red and blue circle represent the data point from the same measurement before and after the correction for FSI. The arrow shows the size of the theoretical correction needed to properly interpret the datum.

reaction mechanism.

1.3.3 Measurement of asymmetry A_1^n

A detailed knowledge of the ground-state spin structure of ^{3}He is essential also for other types of experiments that are considering ^{3}He as an effective polarized neutron target. An example of such experiment is the measurement of the neutron spin asymmetry A_1^n, which is important for understanding the spin structure of the neutron (see Fig. 1.5). In particular, it provides a definitive information about the spin carried by the quarks and gives an insight in to the continuing question of the role of the quark orbital angular momentum in the nucleon wave function [13]. Fig 1.5 shows the error budget of the experiment E99-117 [1, 14, 15] in which asymmetry A_1^n was extracted. The two largest sources of error are the statistical uncertainty and the uncertainty of the polarization of proton (P_p) and neutron (P_n) inside the ^{3}He. These polarizations depend directly on structure of the nuclei and three components of the ground-state wave function. Although the statistical error dominates over the rest of the error con-

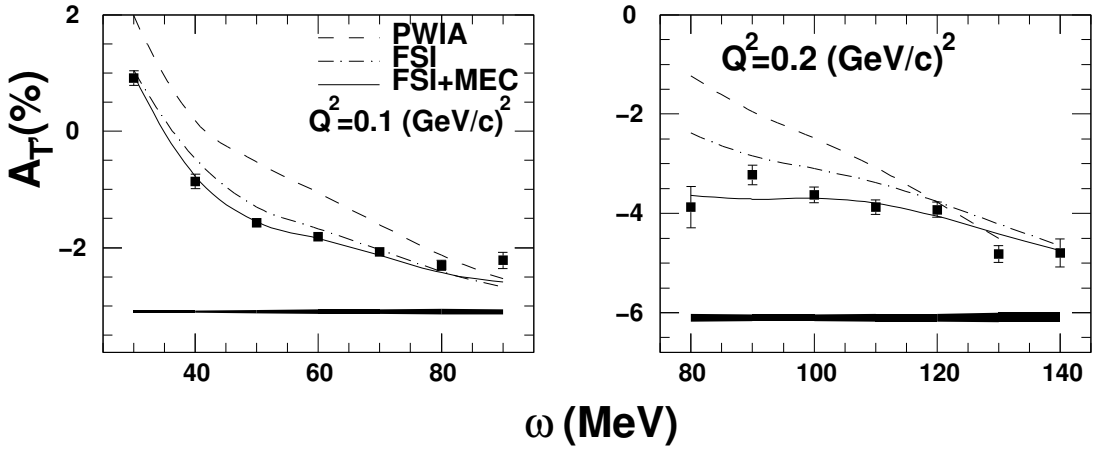

Figure 1.4 — The measured transverse asymmetry $A_{T'}$ in $^3\vec{He}(\vec{e}, e')$ at $Q^2 = 0.1, 0.2\,(GeV/c)^2$ [12]. PWIA calculations are shown as dashed lines. The Faddeev calculations with FSI only and with both FSI and MEC are shown as dash-dotted and solid lines, respectively.

tributions in the E99-117, it is estimated that it will become comparable or even smaller than the uncertainty in P_p and P_n for the upcoming A_1^n experiment E12-06-122, which will be utilizing a polarized ^{3}He with the 11 GeV electron beam. At that point any corrections to P_p and P_n would result in a shift of all points up or down and consequently change the interpretation of the zero crossing of $A_1^n(x)$.
With the increasing statistics, the precision of the current and upcoming double-polarized experiments is reaching a level, that can only be matched by the best theoretical models of the ^{3}He nucleus [1]. These models therefore require progressively more accurate input to adjust their parameters like the ground-state wave-function components, and a complete understating of the spin and isospin dependence of final-state interactions and meson-exchange currents. To achieve this a direct measurement devoted to a better understanding of the ^{3}He itself is needed. Without a significant improvement of this understanding, future experiments on ^{3}He will be seriously impaired [1]. The properties of the ^{3}He need to be studied on a broad kinematic range to create enough lever to constrain the theories.

1.4 Understanding ^{3}He nuclei

1.4.1 Unpolarized experiments

A high level of interest and motivation for understanding the structure and properties of ^{3}He can be recognized in an extensive theoretical and experimental effort to study unpolarized processes $^3\mathrm{He}(e, e'd)$ and $^3\mathrm{He}(e, e'p)$. The MIT-Bates experiment [16] measured reaction $^3\mathrm{He}(e, e'd)p$ at four-momentum transfer $q = 420\,\mathrm{MeV/c}$, for two different proton recoil momenta $p_r = 22$, and $54\,\mathrm{MeV/c}$, in parallel deuteron kinematics. In the region of low proton recoil momentum ($p_r \approx 0$) one would naively expect that the cross-section follows that for the elastic scattering of a free deuteron. Since elastic scattering of a free deuteron chooses isoscalar currents ($T = 0$), one would think

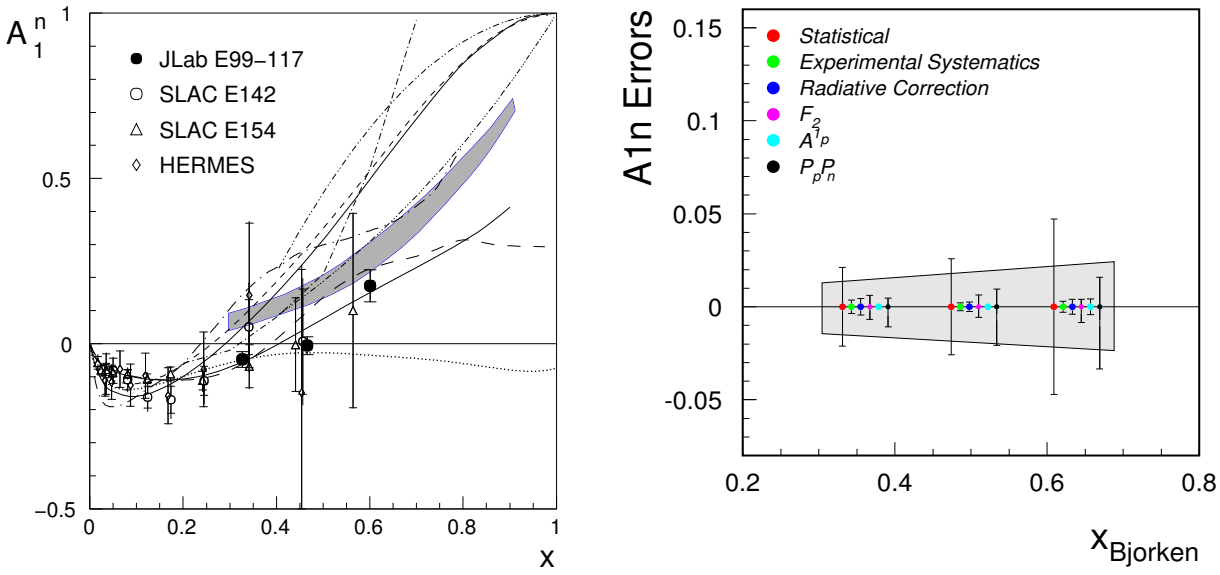

Figure 1.5 — [Left:] The results of the $A_1^n(x)$ measurements, compared to the theoretical predictions [14]. The measurements show a zero crossing around $x = 0.47$ and a significantly positive value at $x = 0.60$. The results at high x agree with the predictions of the constituent quark model but disagree with the predictions of the leading-order perturbative QCD (PQCD). This might indicate, that quarks have non-zero orbital angular momentum [15]. [Right:] Summary of uncertainties in the experiment E99-117. The statistical uncertainty dominates. P_pP_n denotes the error caused by the uncertainty of the polarization of the proton and neutron in $^3\vec{He}$. The light-blue band represents the predicted statistical error of the upcoming experiment E12-06-122. The uncertainty becomes comparable to or even smaller than the error in P_pP_n.

that the dominant mechanism in the two-body (p + d) breakup would also involve the interaction with a correlated $T = 0$ pair, known as a quasi-deuteron model (QDM). However, the two-body currents in the $^3He(e, e'd)p$ reaction contain also the isovector ($T = 1$) components. This experiment has shown, that the $T = 1$ currents play an important role and contributes substantially to the final value of the cross-section (see Fig. 1.6). Hence, $^3He(e, e'd)p$ can not be adequately explained by the QDM, but reaction mechanism containing both isoscalar and isovector currents must be considered.
A Jefferson Lab experiment E89-044 also contributed an important new insight into the characteristics of the ^3He breakup process. In particular, they found an evidence of NN-correlations and demonstrated the importance of the FSI. The $^3He(e, e'p)d$ reaction [17] and $^3He(e, e'p)pn$ reaction [18] were measured at fixed energy and momentum transfers ($\omega = 840\,MeV$ and $|\vec{q}| = 1502\,MeV/c$), and covered a tremendous range of missing momenta up to $1\,GeV/c$, for missing energies up to the pion threshold. These benchmark measurements were much higher in statistics than any previous previous measurement [19]. The experimental data for both, two-body breakup (2bbu) and three-body breakup (3bbu), channels were well described by the approach of Laget [20].
One-body mechanisms, where electron interacts with a single nucleon and deuteron is just a spectator (PWIA), is sufficient to describe $^3He(e, e'p)$ reactions below recoil (missing) momenta $p_r \approx 300\,MeV/c$. In the p_r region between $300\,MeV/c$ and $700\,MeV/c$, nucleon-nucleon final-state interactions become important. Fig. 1.7 shows that the 3bbu cross-section in this region is up to three orders of magnitude larger than the

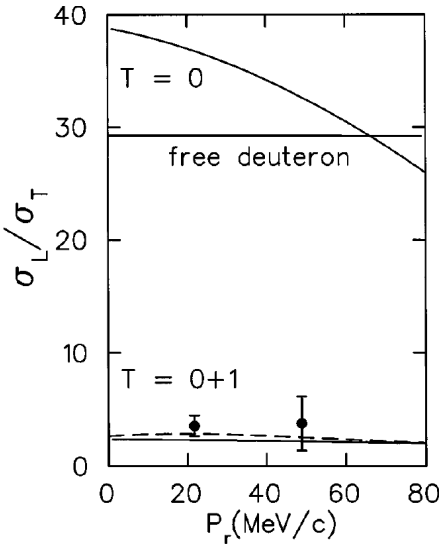

Figure 1.6 — The ratio of the longitudinal and transverse response functions σ_L/σ_T as a function of recoil momentum P_r [16]. The theoretical calculations considering only $T = 0$ currents and both $T = 0$ and $T = 1$ currents are shown with dashed and solid line, respectively. The ratio for the free deuteron is also shown.

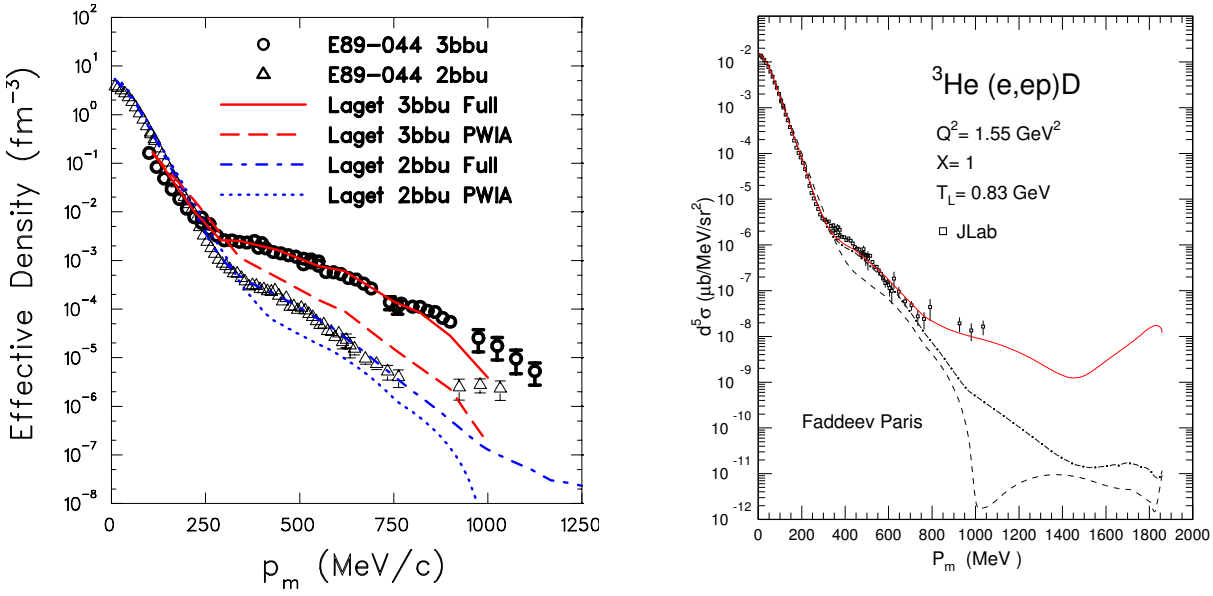

Figure 1.7 — [Left:] Proton effective momentum density distributions in ^{3}He extracted from ^{3}He(e, e′p)d and ^{3}He(e, e′p)pn [18]. Experimental results are compared to the calculations from Laget. PWIA calculations and full Faddeev calculations for each reaction channel are shown with dashed and solid line, respectively. [Right:] Theoretical predictions by Laget [20] for the momentum distribution in reaction ^{3}He(e, e′p)d at $Q^2 = 1.55$ (GeV/c)^2 compared to the JLab data [17]. Dashed line shows the PWIA calculations. Dash-dotted line considers two-body FSI, MEC and Δ production. Full line represents full calculations including also three-body processes.

corresponding 2bbu cross section. This significant difference is caused by a much larger role of FSI and NN-correlations in the 3bbu than in the 2bbu, because of the reduced probability for the two undetected nucleons to recombine and form the ejected deuteron at high p_r. The comparison of PWIA calculations for both reaction channels reveals only one order of magnitude enhancement of the 3bbu over the 2bbu, due to the NN-correlations. The rest is contributed by the FSI and is represented in Fig. 1.7 as a difference between the dashed-line (PWIA calculation) and solid line (full calcula-

tions). The two-orders of magnitude correction to the cross-section contributed by the FSI indicates a great importance of the FSI in the 3bbu of ^{3}He. On the other hand, the two-body processes like meson-exchange currents and formation of Δ, contribute only at level of $\approx$ 20 %. The flattening of the 2bbu cross-section in the p_r region between 700 MeV/c and 1000 MeV/c was explained by the three-body mechanism which dominates there [20]. A virtual photon is absorbed by a nucleon at rest. This nucleon emits meson, which is then absorbed by the the remaining two nucleons [21]. From all this we can see, that experiment E89-044 enabled a simultaneous study and interpretation of one-, two- and three-body mechanisms and significantly enriched our knowledge on the ^{3}He system.

In the case of the deuteron knockout, things are unfortunately not that well understood. An important puzzle is related to the results of the NIKHEF experiment [22], where they measured unpolarized cross-section for the ^{3}He(e, e′d)p reaction as a function of recoil momentum p_r in (q, ω)-constant kinematics. An example of their measurements is shown in Fig. 1.8. To the date, the theory was unable to adequately de-

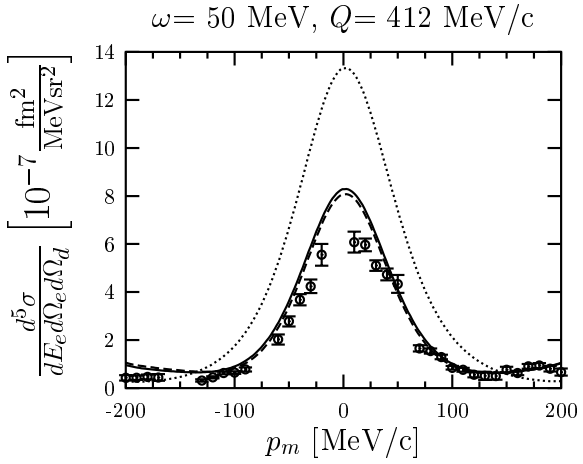

Figure 1.8 — The measured cross-section for ^{3}He(e, e′d)p as a function of proton recoil momentum [22]. Dotted curve represents the results of the PWIAS calculations. Dashed line shows full calculations without MEC. Predictions shown with solid line include also MEC. The PWIA calculations are not shown (totally negligible) [23].

scribe these data. In spite continuous theoretical efforts the inconsistency remains. Even most sophisticated Faddeev calculations, which employ the AV18 nucleon-nucleon interaction and include MEC overestimate the measured cross sections. At present is not clear if this discrepancy is caused by an error in the measurements or by an inadequate theoretical description. Therefore further measurements with greater precision and sensitivity to the theoretical ingredients are needed to resolve these issues [23, 21]. Beam-target asymmetries seem to be very promising candidates for such observables.

1.4.2 Double-polarization experiments

The results from the unpolarized ^{3}He experiments and corresponding theoretical calculations have revealed important information about the structure and properties of the ^{3}He system and have proven the need for full Faddeev calculations. Regrettably, the measurements of the unpolarized cross-section do not have the strength to isolate small components (S′ and D) of the ^{3}He ground-state wave-function which have the ability to further constrain theoretical models. This gives double-polarization observables an important advantage. It has been demonstrated by various theoretical

groups [24, 25, 26, 27], that measurements of beam-target asymmetries in $^3\vec{\mathrm{He}}\,(\vec{e}, e'd)$ and $^3\vec{\mathrm{He}}\,(\vec{e}, e'p)$ can provide precise information on both S′ and D components of the ^{3}He ground-state wave-function.

The use of double-polarization observables has already proven to be very succesful in experiments with polarized ^{2}H. Fig 1.9 shows the results of a NIKHEF experiment [28], where they used deuteron as a benchmark for testing nuclear theory. They

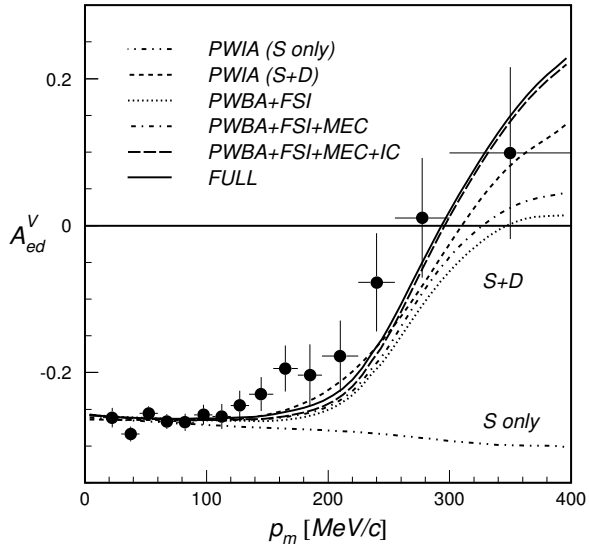

Figure 1.9 — Spin correlation parameter A_{ed}^V in reaction $^2\vec{\mathrm{H}}\,(\vec{e}, e'p)\,n$ as a function of recoil (neutron) momentum at $Q^2 = 0.21\,(\mathrm{GeV/c})^2$. Curves show predictions of different theoretical models. The need for inclusion of the D state into the predictions is clearly demonstrated, since the PWIA with S-state only does not change sign at higher recoil (missing) momenta. Incorporation of FSI, MEC and IC have tendency to move theoretical predictions closer to the experimental values, but do not have power to significantly change results.

measured spin-momentum correlation parameter A_{ed}^V for the $^2\vec{\mathrm{H}}\,(\vec{e}, e'p)\,n$ reaction at $Q^2 = 0.21\,(\mathrm{GeV/c})^2$. The measured data give precise information about the deuteron spin structure and are in good agreement with different theoretical models. Theory predicts that ^{2}H ground-state wave functions is principally combined of two major components. In the dominant S-component are spins of both, proton and neutron, aligned with the spin of the nuclei, while in the D component they are oriented in the opposite direction. There is a $\approx 90\,\%$ probability of finding deuteron in the S-state and $\approx 10\,\%$ probability of finding it in the D state. Fig. 1.9 shows that contribution of D state is essential for obtaining proper description of the experimental data at higher missing momenta. Hence, if ground-state wave function would consist of only S-state, spin correlation parameter A_{ed}^V would have to have significantly different shape. One can also see, that final-state effects become important only at high recoil momenta. Unfortunately, the accuracy of the data in this region becomes poor and obstructs the study of such effects. This speaks in favor of double-polarization measurements with polarized ^{3}He, where significant contributions final-state effects are measurable already at smaller recoil momenta. In addition, ^{2}H does not contain the S′ state, which is dominating the region of small recoil momenta and has a potential to further constrain theoretical models. Such effects can be studied only with ^{3}He, which makes ^{3}He even more exciting playground to test nuclear dynamics.

An important milestone in study of polarization degrees of freedom in ^{3}He was set by the experiment at Indiana University Cyclotron Facility (IUCF) [30]. They determined for the first time spin asymmetries in the momentum distributions of the neutron and proton in ^{3}He. The measured asymmetries in quasi-elastic processes $^3\vec{\mathrm{He}}(\vec{p}, 2p)$ and

$^3\vec{\mathrm{He}}(\vec{p}, pn)$ were compared to the PWIA calculations. They observed a good agreement of the measurements with the theory. A 100 % asymmetry in the momentum distribution of the neutron at low momenta demonstrated a strong dominance of the S state in the ^{3}He ground-state wave-function and provided confidence, that ^{3}He can be used as an effective polarized neutron target for scattering experiments in nuclear and particle physics. On the other hand, the observed negative asymmetry ($\approx -15\,\%$) in the momentum distribution of a proton was interpreted as an indication for the presence of the S′-state. However, this interpretation might be misleading, since their calculations have not considered effects such as FSI, which in general have the ability to substantially change the final value of the asymmetry.

The IUCF experiment also revealed the weaknesses inherent to the use of hadronic probes and helped to initiate a study of spin-dependent momentum distributions in ^{3}He with the use of electrons. being a point-like particles, electrons represent the cleanest probe for testing nuclear structure and can provide much better resolving power than hadrons. Hence, the effort for disentangle the effects of small wave-function components has shifted to electro-disintegration of polarized ^{3}He.

The pilot measurement of beam-target asymmetries, utilizing a ^{3}He target in combination with polarized electron beam, was performed at NIKHEF [29], where they determined the A_z asymmetry in $^3\vec{\mathrm{He}}\,(\vec{e}, e'p)$ and $^3\vec{\mathrm{He}}\,(\vec{e}, e'n)$ reactions at beam energy of 442 MeV and at $Q^2 = 0.16\,(\mathrm{GeV/c})^2$. They obtained a small value of the asymmetry in the proton channel ($A_z = 0.15 \pm 0.11$), but a large value in the neutron channel ($A_z = -0.56 \pm 0.18$). This was in agreement with the theoretical predictions where the main contribution of the ^{3}He wave-function represents the spatially symmetric S-state, where the protons occupy a spin-singlet state and neutron caries the majority of ^{3}He spin. Although this measurement was low in statistics, it already demonstrated the feasibility of the double-polarization experiments at medium beam energies (≈ 1 GeV), indicated the need for full Faddeev calculations and laid the ground work for further experiments.

Polarization degrees of freedom were successfully utilized in the MAINZ experiment [31] for studying meson-exchange currents and final-state interactions in the ^{3}He breakup process. They measured beam-target asymmetries A_z and A_x in both $^3\vec{\mathrm{He}}\,(\vec{e}, e'p)\,d$ and $^3\vec{\mathrm{He}}\,(\vec{e}, e'p)\,pn$ reactions. The measurements were performed at the top of the quasi-elastic peak at $Q^2 = 0.3\,(\mathrm{GeV/c})^2$, with $\omega = 135$ MeV and $|\vec{q}| = 570$ MeV/c. According to Faddeev calculations for this kinematic conditions, MEC effects should be small. On the other hand, calculation predict very distinct roles of FSI in the 2bbu and 3bbu processes. In the 2bbu channel, the PWIA asymmetry and the asymmetry including FSI are almost identical. However, in the 3bbu case, the PWIA asymmetry is almost exactly zero, implying the usual picture of a spin-singlet proton-proton pair (see Fig. 1.1), while the asymmetry including FSI is large and negative [21]. The measured results are shown in Fig. 1.10 and they agree well with the computed values.

Mainz experiment unfortunately provided data only at low recoil momenta ($p_r \leq 120$ MeV/c). They also performed no binning of the datum the in the p_r variable. All their data were collected in one bin with the mean value of $p_r \approx 40$ MeV/c. Furthermore, they measured asymmetries only in $^3\vec{\mathrm{He}}\,(\vec{e}, e'p)$ reaction, while the deuteron

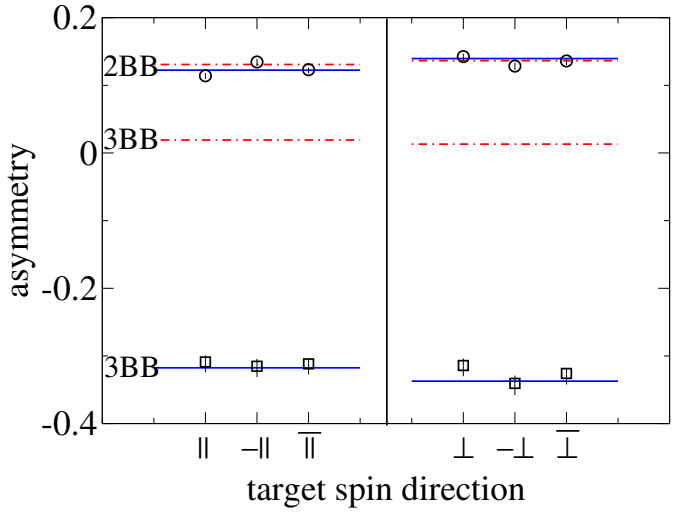

Figure 1.10 — Measured longitudinal A_z and transverse A_x asymmetries for 2BBU reaction channel $^3\vec{\mathrm{He}}\,(\vec{e},e'p)\,d$ and 3BBU reaction channel $^3\vec{\mathrm{He}}\,(\vec{e},e'p)\,pn$. Symbols $\|$, -$\|$, $\perp$ and -$\perp$ denote four target spin orientations: parallel to $\vec{q}$, anti-parallel, perpendicular and anti-perpendicular. The symbols $\overline{\|}$ and $\overline{\perp}$ represent the mean value of the asymmetry in each direction. Dash-dotted and full line represent PWIA and full theoretical predictions for 2BBU and 3BBU, respectively [31].

channel $^3\vec{\mathrm{He}}\,(\vec{e},e'd)$ remains unexplored. Hence, new measurements are required, similar to those from NIKHEF [28], to obtain double-polarization asymmetries as a function of recoil momentum in all reaction channels, which could reveal the presence of S'- and D-state in the ^{3}He ground-state wave-function. The first attempt of such measurement was performed in NIKHEF [32]. However, the statistical accuracy of those measurements was insufficient to resolve the role of S' component at low recoil momenta. Therefore their results were never published. This way E05-102 is the first experiment, where S'- and D-wave contributions to the ^{3}He wave-function will be inspected in most direct manor. With these ground breaking measurements we will be able to confirm or reject theoretical predictions on spin and iso-spin structure of the nuclei and re-examine our understanding of the meson exchange currents and final state interactions.

1.5 Experiment E05-102

Experiment E05-102 is the only polarized ^{3}He experiment carried out at Jefferson Lab which is seeking to better understand the ^{3}He system, by measuring beam-target asymmetries A_x and A_z in reactions $^3\vec{\mathrm{He}}\,(\vec{e},e'd)$ and $^3\vec{\mathrm{He}}\,(\vec{e},e'p)$. The asymmetries were measured for recoil momenta p_{Miss} between 0 and almost 300 GeV/c. In this kinematics range $(e,e'd)$ channel is predicted to be uniquely sensitive to the effects of both S' and D components of the ^{3}He ground-state wave function. Fig. 1.11 shows the calculated values of the asymmetries, made for kinematic settings very similar to those during the E05-102 experiment. An important role of the S'-state is evident at small recoil momenta, where asymmetry seems to be relatively flat and independent of the p_r. In this region a potential absence of the S'-state would cause almost a 30 % change in the asymmetry. The contribution of the D-component becomes significant at larger $p_r > 120$ MeV/c, with asymmetry starting to change dramatically.

When looking at the double-polarized asymmetries in $^3\vec{\mathrm{He}}\,(\vec{e},e'p)$, one has to consider that two reaction channels $^3\vec{\mathrm{He}}\,(\vec{e},e'p)\,d$ and $^3\vec{\mathrm{He}}\,(\vec{e},e'p)\,pn$ are possible. The experimental setup of the experiment E05-102 allowed simultaneous measurement of both

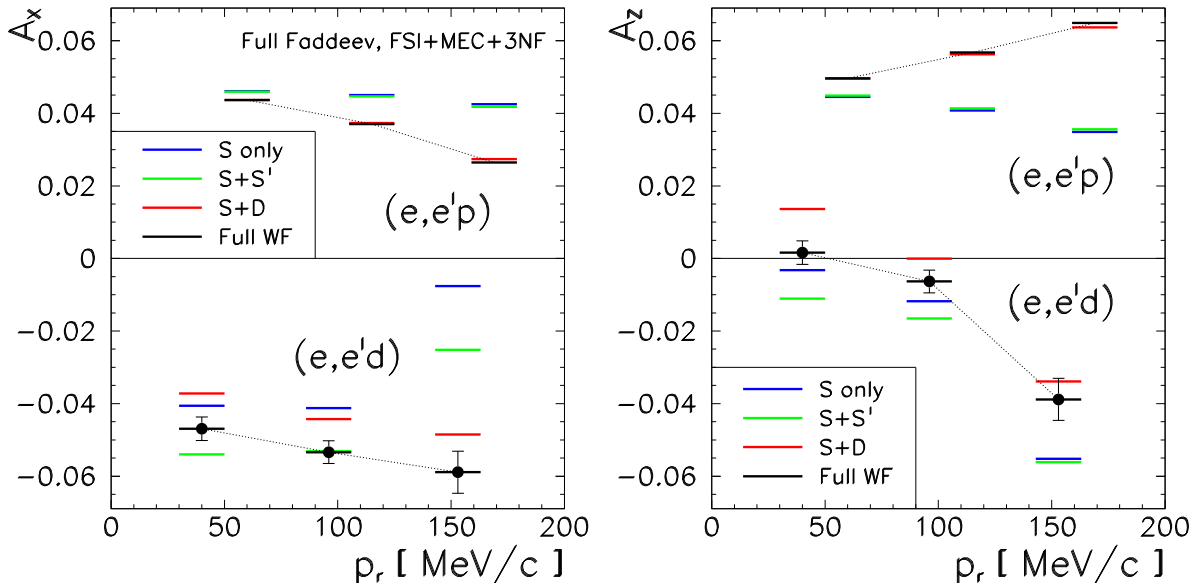

Figure 1.11 — Asymmetries Ax and Az in processes $^3\vec{\mathrm{He}}\,(\vec{e}, e'd)\,p$ and $^3\vec{\mathrm{He}}\,(\vec{e}, e'p)\,d$ for a beam energy of 2.4 GeV and $|\vec{q}| = 620\,\mathrm{MeV/c}$ predicted by Golak [1]. Asymmetries depend on the S' and D components of the ^{3}He ground-state wave function. The relative influence of each component changes with the recoil momentum p_r. Measurement of double-polarized asymmetries therefore represents a valuable technique for studying properties of ^{3}He.

channels. Measured asymmetries are this way linear combinations of contributions from both channels. This has to be acknowledged when data are compared to the theoretical calculations. The predicted asymmetries for the two-body-breakup (2BBU) are presented in Fig. 1.11. It is believed that this channel is sensitive only to the D-state, while the contributions of the S' state are negligible. Here, asymmetry is also predicted to be reasonably flat for small recoil momenta and starts decreasing when $p_r > 120\,\mathrm{MeV/c}$. This behavior is again governed by the D-state.
The properties of final state interactions and meson exchange currents are also unmasked through the measurement of A_x and A_z asymmetries. This was indicated already by Laget [33]. Within the framework of plain-wave impulse approximation (PWIA) he demonstrated, that inclusion of such effects can dramatically change the final value of the asymmetries in $(e, e'p)d$ and $(e, e'p)pn$ reactions. See Fig. 1.12 for the details. FSI and MEC contributions are different in each reaction channel, and in general can not be neglected. This gives an excellent opportunity to study FSI and MEC via double-polarized asymmetries on 3He target.

The predictions for observables A_x and A_z based on the non-relativistic Faddeev calculations are provided by various theoretical groups. In the last few years, all groups made major theoretical advances, especially in the treatment of the meson exchange currents and three nucleon force. Their calculations have been cross-checked in many instances [1]. However, in some aspects there are still significant differences between them. Fig. 1.13 shows the comparison of the state-of-the-art predictions of Bochum/Krakow and Hannover groups for $^3\vec{\mathrm{He}}\,(\vec{e}, e'd)\,p$. Differences in predictions are marked in both asymmetries, especially in the case of longitudinal asymmetry. The conclusive results from the direct measurements of A_x and A_z will put these competing theoretical calcu-

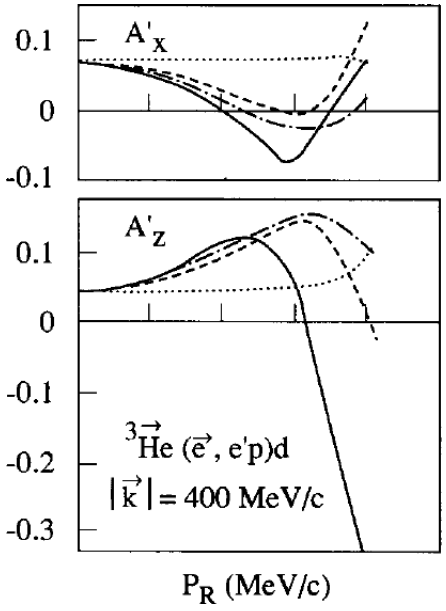

Figure 1.12 — Asymmetries A_x and A_z in the reaction $^3\vec{\text{He}}\,(\vec{e}, e'p)\,d$ as a function of recoil momentum p_r for parallel kinematics ($\vec{p_r} \parallel \vec{q}$) at a beam energy of 880 MeV. The dotted lines and dashed lines correspond to the PWIA when only S-wave and both S- and D-waves are respectively taken into account. The dash-dotted lines include FSI, while full lines include also MEC [33].

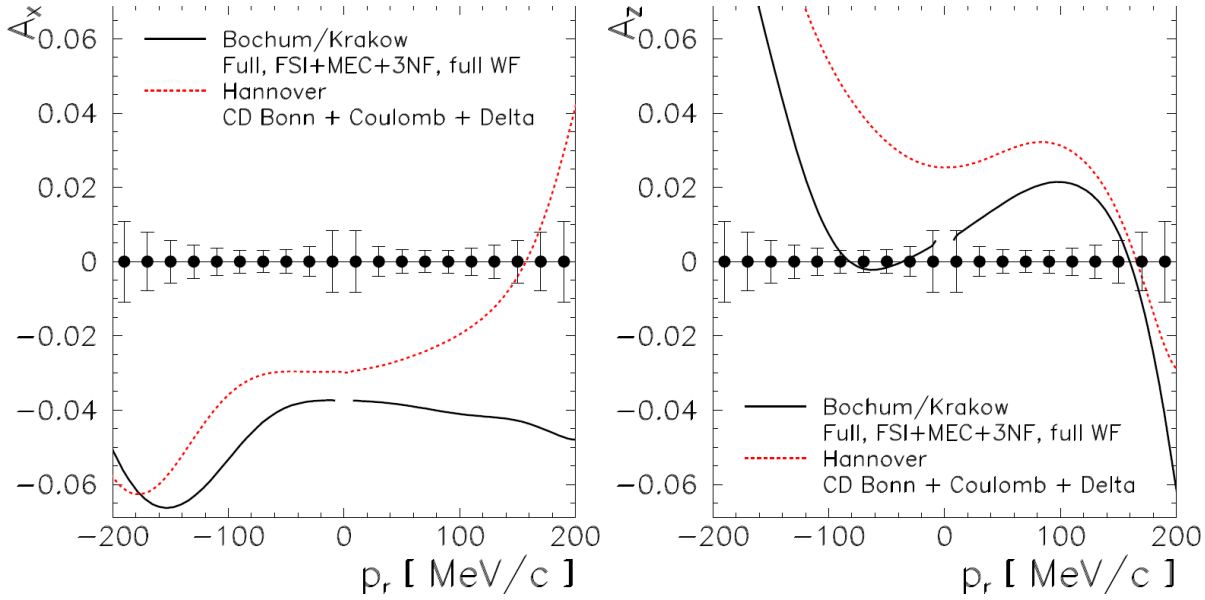

Figure 1.13 — Comparison of predicted double-polarized asymmetries A_x and A_z provided by Bochum/Krakow and Hannover group. A significant discrepancy between two calculations is observed for the longitudinal asymmetry A_z. Figure taken from [1].

lations to the test and help significantly in diminishing the differences between them.

1.6 This work

In this thesis I will study the spin-isospin structure of the polarized ^{3}He, through the analysis of double-polarization asymmetries, measured in the experiment E05-102. The data for all three reaction channels $^3\vec{\text{He}}\,(\vec{e}, e'd)\,p$, $^3\vec{\text{He}}\,(\vec{e}, e'p)\,d$ and $^3\vec{\text{He}}\,(\vec{e}, e'p)\,pn$ will be inspected in order to get new insight into the properties of the ^{3}He. Within

the limits of this work all open questions, discusses in this chapter, will not answered. However, the results obtained from these ground breaking measurements with contribute extensively to our knowledge on the structure of the ^{3}He and accompanying reactions effects. The high precision data, covering wide range of recoil momenta (up to $\approx 300\,\mathrm{MeV/c}$) at different Q^2, will allow us to confirm or reject the theoretical predictions on the spin and iso-spin structure of the nuclei and check our understanding of the meson exchange currents and final state interactions. Without this knowledge all future experiments on ^{3}He at low Q^2 will be seriously impaired.

The thesis will be divided in following sections. First, the underlying theoretical formalism will be briefly explained. Numerical predictions provided by different theoretical groups will be presented and compared. Next, the apparatus utilized for the experiment E05-102 will be described, followed by the chapter about the calibration of spectrometers and detectors. A special attention will be dedicated to the optical calibration of the BigBite spectrometer, which I commit a lot of time to. After the calibration chapters, systematic and statistic uncertainties will be determined. This will be followed by the main chapter of this thesis, where final experimental asymmetries will be presented and compared to the theoretical calculations. Pursuing chapter will be devoted to interpretation and discussion of obtained results. Finally, summary of the main findings will be presented, followed by the outlook for future work.